eLIFE elifesciences.org

RESEARCH ARTICLE

Figures and figure supplements

Modularity and determinants of a (bi-)polarization control system from free-living and obligate intracellular bacteria

Matthieu Bergé *et al*

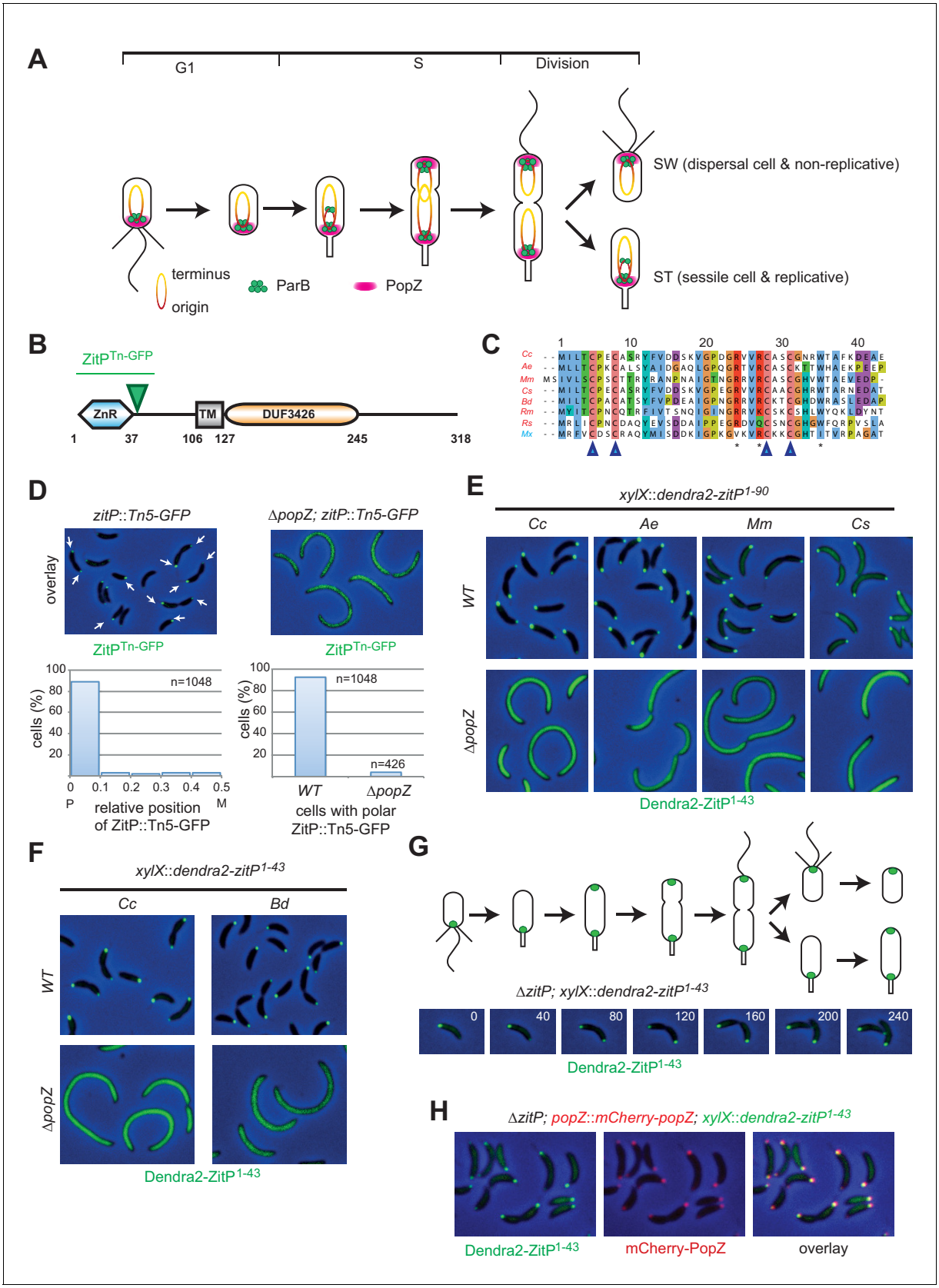

Figure 1. The Zinc finger (ZnR) of ZitP and orthologs is a polar localization signal. (**A**) Schematics of PopZ and ParB localization and chromosome organization during the *C. crescentus* cell cycle. Each cell cycle yields two different daughter cells: a swarmer (SW) and a stalked (ST) cell residing in G1-

Figure 1 continued on next page

Figure 1 continued

and S-phase, respectively. The replication origin region (red, including the centromeric sequence eight kbp from the origin) and the terminus region (yellow) are shown. (**B**) Schematic of the domain organization in ZitP: the N-terminal zinc-finger domain (ZnR), the transmembrane domain (TM) and the C-terminal domain-of-unknown function (DUF3426). The green arrowhead points to the codon in the *zitP* coding sequence harboring the GFP insertion in the *zitP*::*Tn5-GFP* strain. All regions are drawn to scale. Numbers indicate residues. (**C**) Alignment of the ZnR from α-proteobacterial ZitP orthologs (in red) and one δ-proteobacterium (in blue) (accession nos.: YP_002517671 [Cc, *Caulobacter crescentus*], ADU14901 [Ae, *Asticcacaulis excentricus*], ABI66665 [Mm, *Maricaulis maris*], ADG11315 [Cs, *Caulobacter segnis*], WP_003168465 [Bd, *Brevundimonas diminuta*], WP_014365322 [Rm, *Rickettsia massiliae*], WP_011909408 [Rs, *Rhodobacter sphaeroides*] and ABF87224 [Mx, *Myxococcus xanthus*]). The four cysteine residues coordinating the zinc ion are highlighted (blue arrowheads). Asterisks indicate the conserved residues promoting ZitP•PopZ complex formation. (**D**) Overlays of fluorescence and phase contrast images showing the subcellular localization of $ZitP^{Tn\text{-}GFP}$ encoded by the *zitP*::Tn*5-GFP* allele in *WT* or Δ*popZ C. crescentus* cells (top). The graphs below show the quantitation of the localization from above. The left graph indicates the distribution of foci along the longitudinal axis. Focus (n = 1048) position is given in relative coordinates from 0 (pole) to 0.5 (midcell). P, pole; M, midcell. The right graph shows the percentage of cells containing at least one focus of $ZitP^{Tn\text{-}GFP}$ in *WT* (n = 1048) or in Δ*popZ* cells (n = 426). (**E**) Overlay images as in D showing the subcellular localization of the first 90 residues of ZitP from *C. crescentus* (Cc) and orthologs from *A. excentricus* (Ae), *M. maris* (Mm), *C. segnis* (Cs) in *C. crescentus WT* (upper panels) or Δ*popZ* (bottom panels) cells. Strains expressing Dendra2-$ZitP^{1\text{-}90}$ from the chromosomal *xylX* locus were induced with xylose for 4 hr before imaging (phase contrast and Dendra2-fluorescence). (**F**) Overlay images as in D showing the subcellular localization of the ZnR of ZitP (Dendra2-$ZitP^{1\text{-}43}$) of *C. crescentus* (Cc) and orthologs from *B. diminuta* (Bd) in *WT* (upper panels) or Δ*popZ* (bottom panels) *C. crescentus* cells. Strains expressing Dendra2-$ZitP^{1\text{-}43}$ from the chromosomal *xylX* locus were induced with xylose for 4 hr before imaging (phase contrast and Dendra2-fluorescence). (**G**) Time-lapse imaging of swarmer cells from Δ*zitP* cells expressing Dendra2-$ZitP^{1\text{-}43}$ from the chromosomal *xylX* locus after induction for 1 hr with 0.3% xylose. Cells were then synchronized and transferred onto an agarose pad containing 0.3% xylose (t = 0 min), and visualized at 40 min intervals (time in minutes is indicated in the images) by phase contrast and Dendra2-fluorescence microscopy, respectively. Shown above the overlays are the schematics representing $ZitP^{1\text{-}43}$ localization during the *C. crescentus* cell cycle. (**H**) Images of Δ*zitP* cells expressing Dendra2-$ZitP^{1\text{-}43}$ from the chromosomal *xylX* locus and mCherry-PopZ from the native chromosomal *popZ* locus. Fluorescence and phase contrast images were acquired after 4 hr of induction with 0.3% xylose. Cells expressing Dendra2-$ZitP^{1\text{-}43}$ (left panel, green) and mCherry-PopZ (middle panel, red) are shown. Co-localized red and green foci appear yellow in the overlay (right panel).

DOI: 10.7554/eLife.20640.002

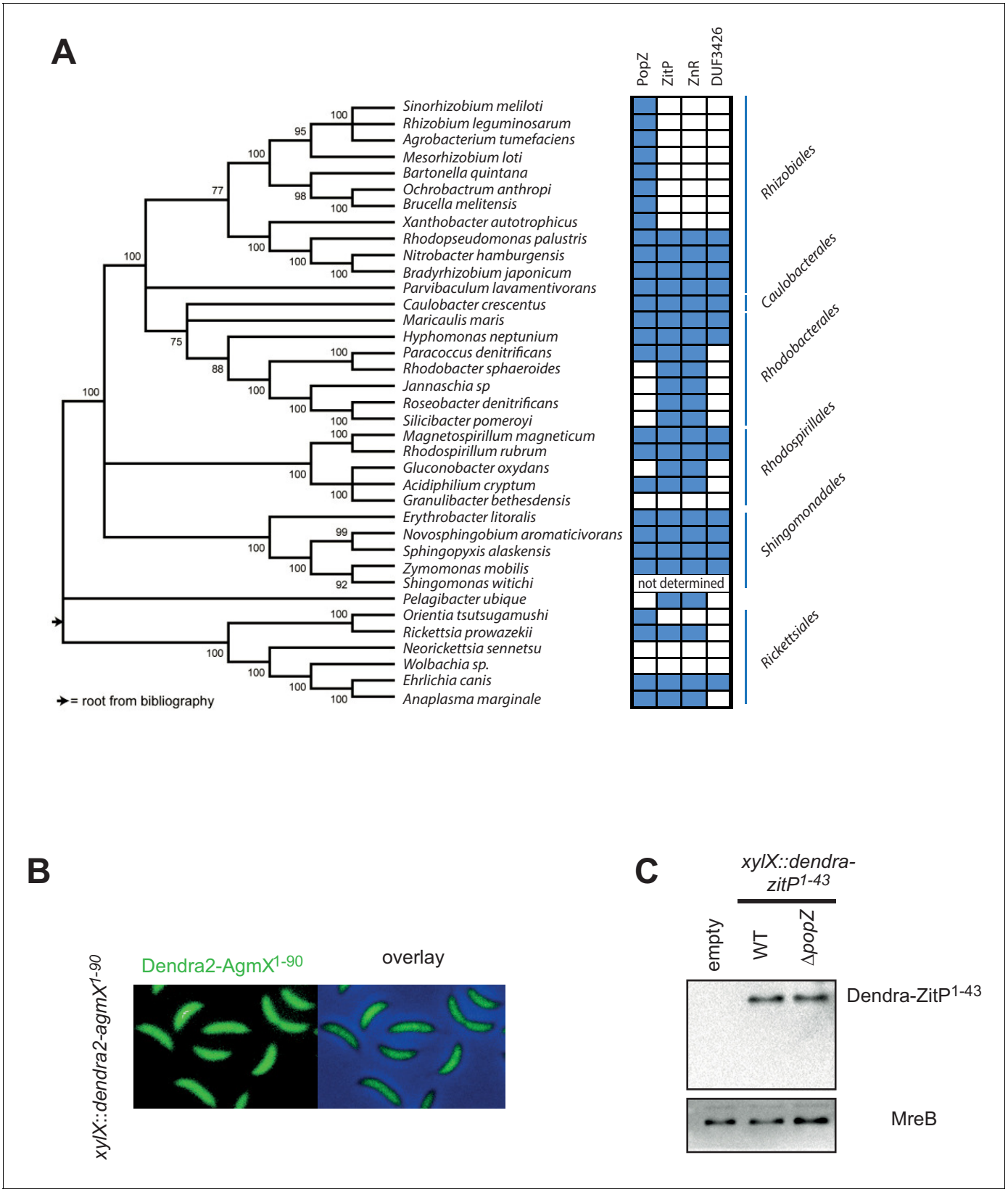

Figure 1—figure supplement 1. Conservation of ZitP and PopZ. (**A**) Distribution of PopZ-, ZitP-, ZnR- and DUF3426-encoding sequences in various α-proteobacterial orders. A 5000-residue long concatamer of universal proteins used to create the phylogeny based on the Neighbor-Joining method with a Dayhoff evolutionary model and 100 bootstrap replicates by Brilli et al. (***Brilli et al., 2010***) was modified. Blue and white boxes indicate the

Figure 1—figure supplement 1 continued on next page

Figure 1—figure supplement 1 continued

presence or absence of orthologs as identified by bi-directional BLASTP searches. (**B**) AgmX from *M. xanthus* is not polarly localized in *C. crescentus*. Subcellular localization of the AgmX ZnR (encoded in the δ-proteobacterium *M. xanthus*) expressed form the *xylX* locus in *WT C. crescentus* cells. Dendra2-fluorescence (left panels) and overlay between phase and Dendra2-fluorescence and phase channel (right panels) are shown. Synthesis of the Dendra2-AgmX$^{1-90}$ was induced for 4 hr with 0.3% xylose before imaging. (**C**) Immunoblots showing the abundance of the Dendra2-ZitP$^{1-43}$ in WT or Δ*popZ C. crescentus* cells. Expression of Dendra2-ZitP$^{1-43}$ integrated at the chromosomal *xylX* locus was induced during 4 hr by the addition of 0.3% xylose. The abundance of Dendra2-ZitP$^{1-43}$ in *WT* or Δ*popZ* cells was monitored using antibodies to Dendra2 (top) or MreB (bottom) as a loading control. A strain that does not express Dendra2 was used as a negative control (empty).

DOI: 10.7554/eLife.20640.003

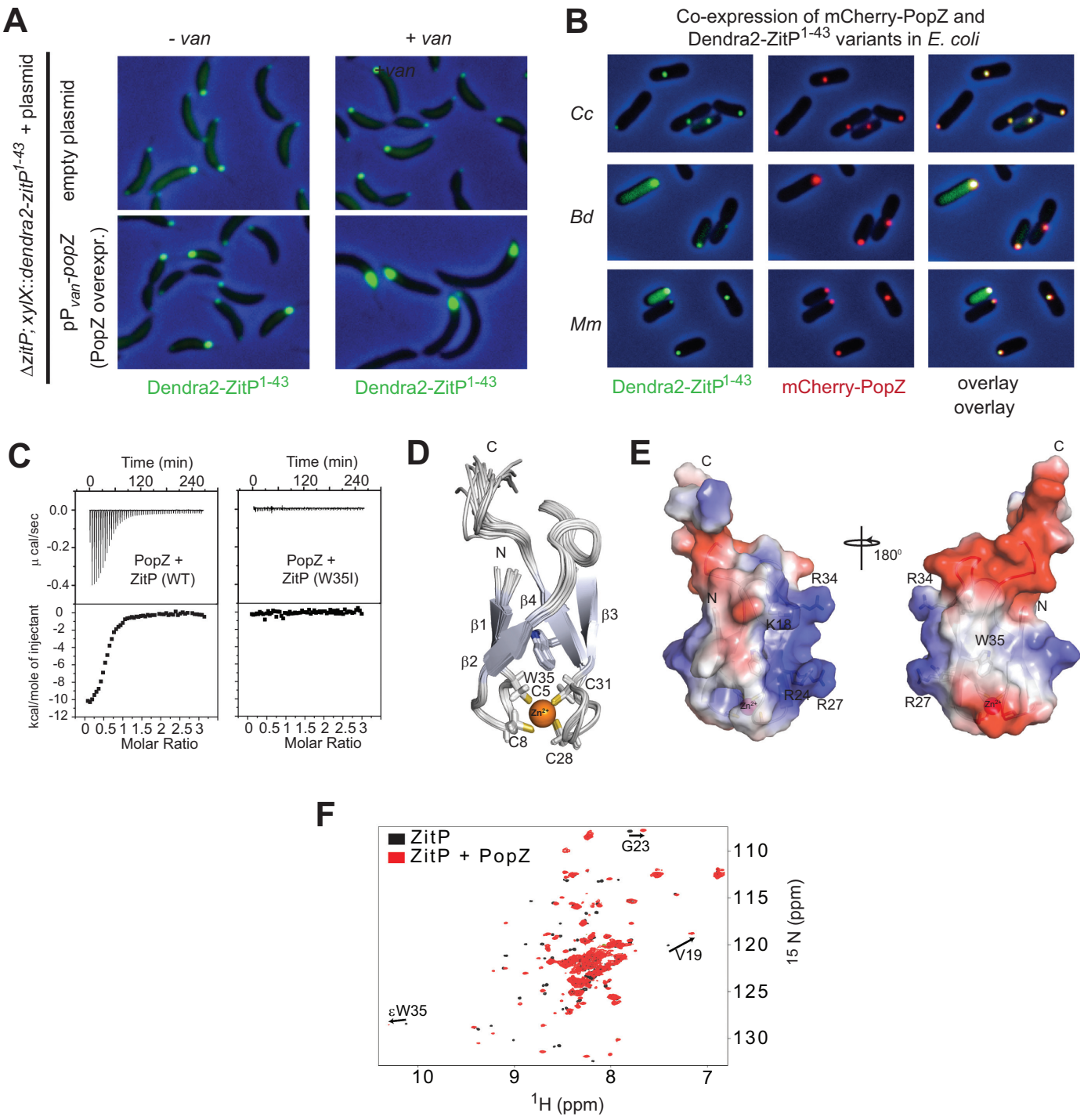

Figure 2. The ZnR of ZitP directly interacts with PopZ. (**A**) Images showing the localization of Dendra2-ZitP$^{1-43}$ in Δ*zitP* cells harbouring the empty vector (upper panel) or a plasmid to overproduce PopZ under control of the vanillate-inducible P_{van} promoter (lower panel). Images were taken before (- van) or after PopZ overexpression was induced by the addition of 0.5 mM vanillate for 5 hr (+ van). (**B**) Images of *E. coli* TB28 cells co-expressing Dendra2-ZitP$^{1-43}$ from *C. crescentus* (Cc), *B. diminuta* (Bd) or *M. maris* (Mm) and mCherry-PopZ. The Dendra2-fluorescence (green channel, right), the mCherry-fluorescence (red, middle) or the combined fluorescence (yellow) channels are shown as overlays with phase contrast images. Cells were grown in LB media for 2 hr, then Dendra2-ZitP$^{1-43}$ variants were induced with 1 mM IPTG and mCherry-PopZ was induced with 0.2% L-arabinose for 2

Figure 2 continued on next page

Figure 2 continued

hr. (**C**) Isothermal titration calorimetry experiments (upper) measuring changes upon injection of 4 µL of a 300 µM PopZ solution into a 15 µM solution of $ZitP^{1-43}$ (left panel) or $ZitP^{1-43W35I}$ (right panel). (Lower) Plot showing the integrated heat changes following each injection as a function of the molar ratio of PopZ to $ZitP^{1-43}$ (left panel) or $ZitP^{1-43W35I}$ (right panel). (**D**) Stereo view of the NMR solution structure of $ZitP^{1-43}$. The secondary structure elements, the cysteine residues coordinating the zinc ion and W35 are indicated. (**E**) Electrostatic surface potential representation of $ZitP^{1-43}$. Several residues in the basic patch are labelled. (**F**) Overlay of the 2D ^{1}H-^{15}N TROSY HSQC spectra of $ZitP^{1-43}$ (black spectrum) or $ZitP^{1-43}$ in complex with PopZ (red spectrum). Black arrows indicate spectroscopic shifts/appearance of new species.

DOI: 10.7554/eLife.20640.004

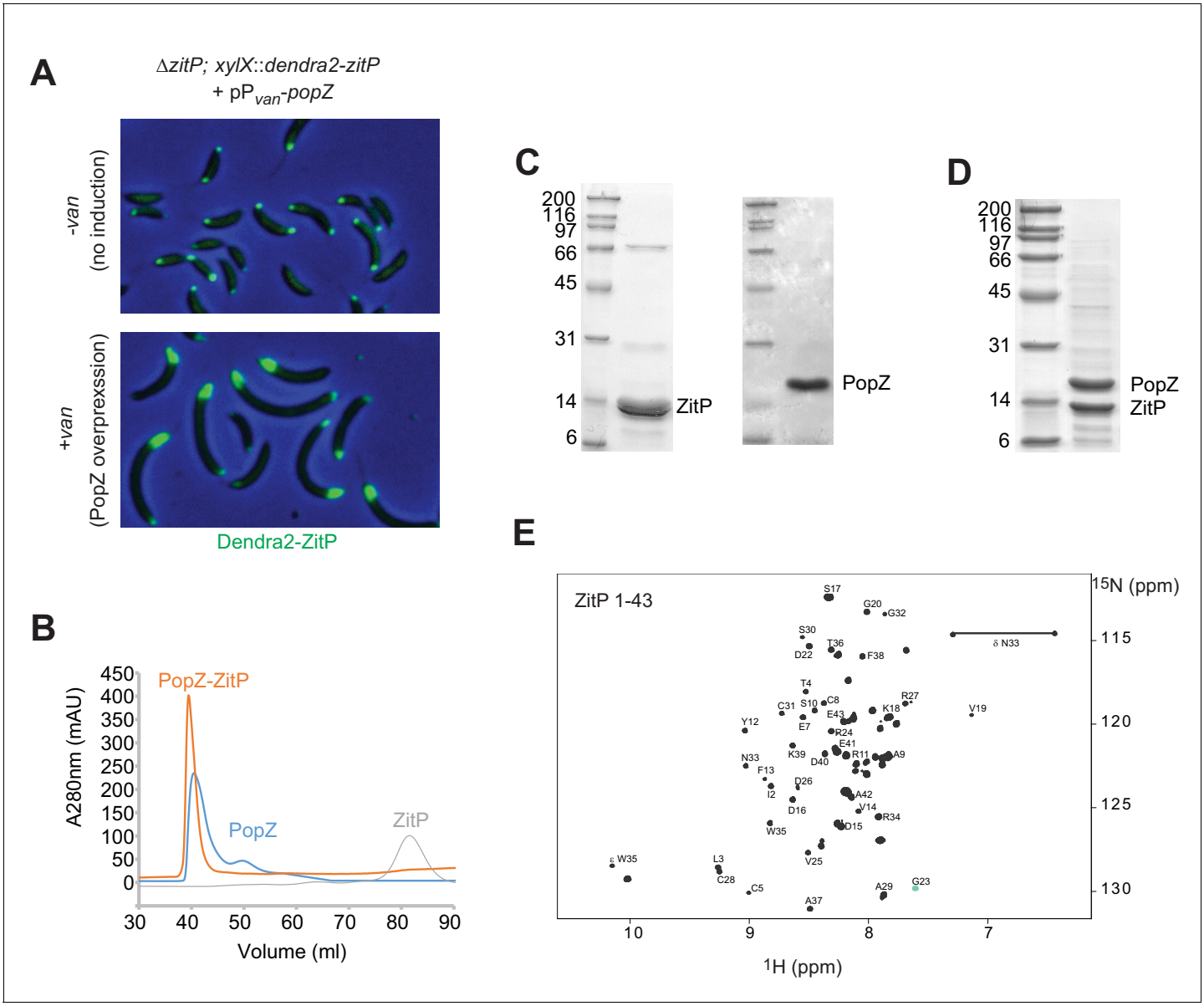

Figure 2—figure supplement 1. Purification of ZitP and PopZ. (**A**) Overlays of Dendra2-fluorescence with phase contrast images of *C. crescentus* cells expressing Dendra2-ZitP from the *xylX* locus without PopZ overproduction (-van, top panel) or with PopZ overproduction (+van. lower). To achieve PopZ expression, cells were induced with in 0.5 mM vanillate for 5 hr prior to imaging. (**B**) Chromatograms of the size exclusion chromatography (SEC) experiments performed on superdex S75 in the NMR buffer with purified His_6-tagged PopZ alone or incubated with one molar equivalent $ZitP^{1-43}$ shown in blue and orange respectively. PopZ alone elutes already as a high molecular weight oligomer. Using these experiments, we found that ZitP co-purifies with PopZ in agreement with the NMR data and the ITC data. (**C**) SDS-PAGE analysis of the PopZ elution peak. Numbers indicate the molecular masses in kDa. (**D**) SDS-PAGE analysis of the PopZ-ZitP elution peak. Numbers indicate the molecular masses in kDa. (**E**) 2D 1 H-15N HSQC spectrum of $ZitP^{1-43}$.

DOI: 10.7554/eLife.20640.005

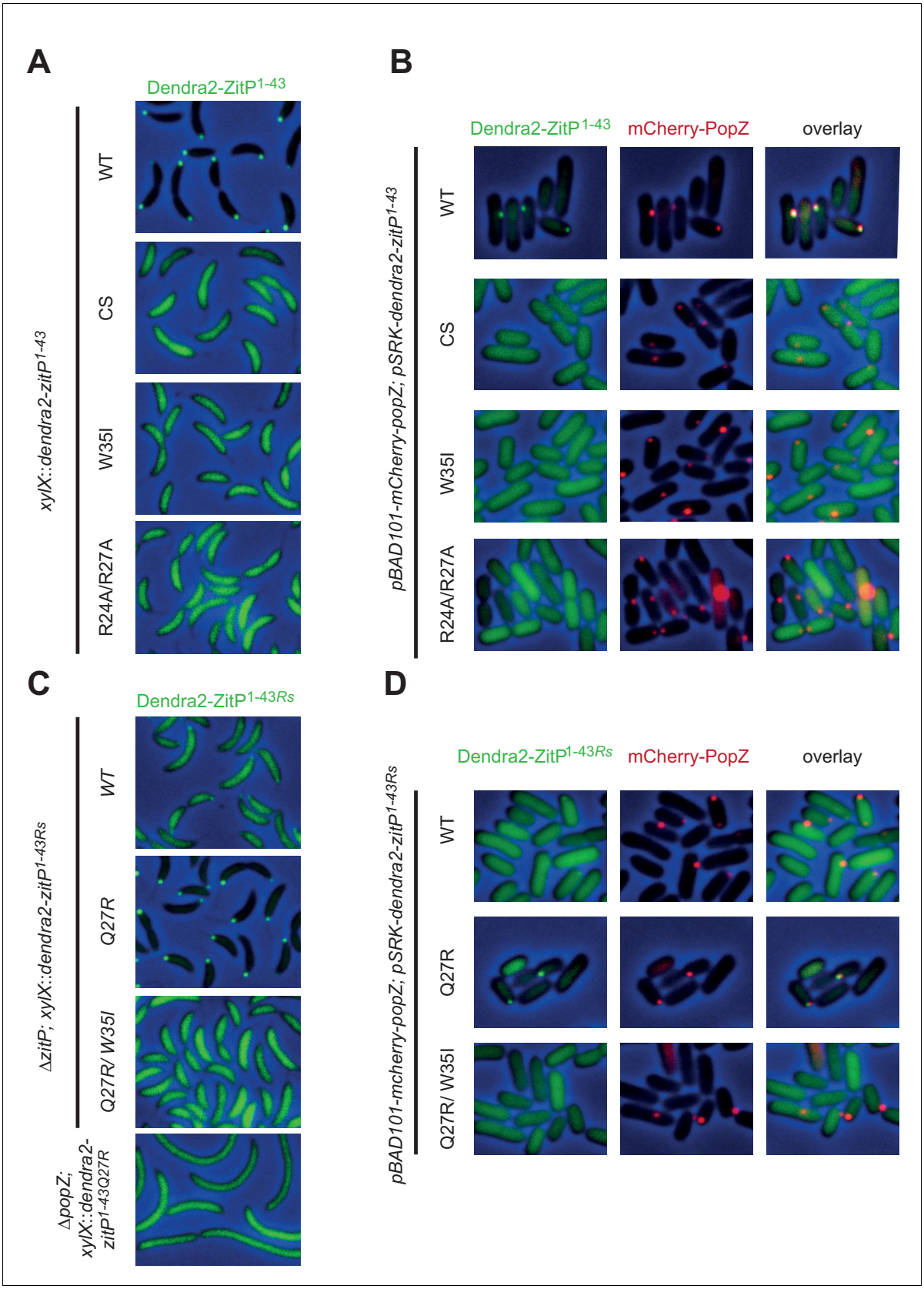

Figure 3. Molecular determinants underpinning the ZitP•PopZ complex. (**A**) Images showing the subcellular localization of *WT C. crescentus* cells expressing Dendra2-ZitP$^{1-43(WT)}$, Dendra2-ZitP$^{1-43(CS)}$, Dendra2-ZitP$^{1-43(W35I)}$ or Dendra2-ZitP$^{1-43(R24A/R27A)}$ from the *xylX* locus. Synthesis of the Dendra2-

Figure 3 continued on next page

Figure 3 continued

ZitP$^{1-43}$ variants was induced with xylose for 4 hr before phase contrast and Dendra2-fluorescence imaging. (**B**) Images of *E. coli* TB28 cells expressing Dendra2-ZitP$^{1-43(WT)}$, Dendra2-ZitP$^{1-43(CS)}$, Dendra2-ZitP$^{1-43(W35I)}$ or Dendra2-ZitP$^{1-43(R24A/R27A)}$ (left panels) in the presence of mCherry-PopZ (middle panels). Overlays between green (Dendra2) and/or red (mCherry) fluorescence and phase contrast images are shown (right panels). Cells were grown in LB for 2 hr, then the expression of Dendra2-ZitP$^{1-43}$ variants and of mCherry-PopZ was induced with 1 mM IPTG and 0.2% L-arabinose, respectively, for 2 hr. (**C**) Images of *WT C. crescentus* cells expressing *R. sphaeroides* (Rs) Dendra2-ZitP$^{1-43(WT)}$, Dendra2-ZitP$^{1-43(Q27R)}$ or Dendra2-ZitP$^{1-43(Q27R/W35I)}$ and of Δ*popZ C.* crescentus cells expressing *R. sphaeroides* Dendra2-ZitP$^{1-43(WT)}$. Synthesis of the Dendra2-ZitP$^{1-43}$ variants was induced from the *xylX* locus 4 hr before phase contrast and Dendra2-fluorescence imaging. (**D**) Images of *E. coli* TB28 cells expressing *R. sphaeroides* (Rs) Dendra2-ZitP$^{1-43(WT)}$, Dendra2-ZitP$^{1-43(Q27R)}$ or Dendra2-ZitP$^{1-43(Q27R/W35I)}$ (left panels) in the presence of mCherry-PopZ (middle panels). Overlays between green (Dendra2) and/or red (mCherry) fluorescence channels with phase contrast images are shown (right panel). Cells were grown in LB for 2 hr, then the expression of Dendra2-ZitP$^{1-43}$ variants and of mCherry-PopZ was induced with 1 mM IPTG and 0.2% L-arabinose, respectively, for 2 hr.

DOI: 10.7554/eLife.20640.006

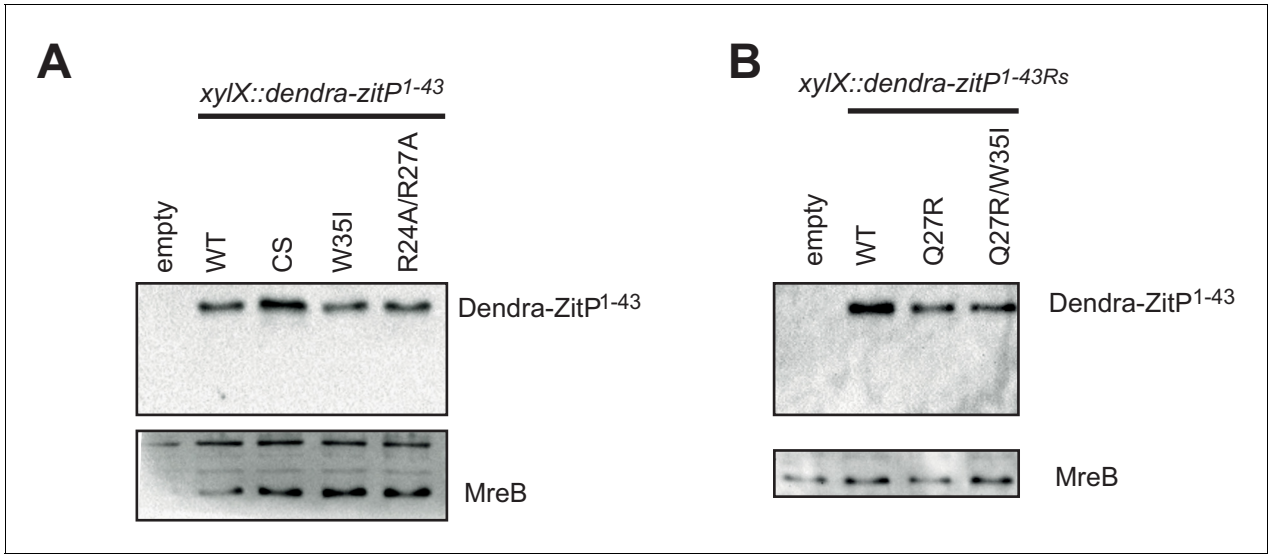

Figure 3—figure supplement 1. Steady-state levels of Dendra-ZitP$^{1-143}$ variants. (**A**) Immunoblots using antibodies to Dendra2 (top) or MreB (bottom, loading control) showing the abundance of Dendra2-ZitP$^{1-43}$ variants in *C. crescentus WT* strains. Expression of Dendra2-ZitP$^{1-43}$ variants (CS: C5S/C8S/C28S/C31S quadruple; W35I and R24A/R27A double mutants) was induced from the *xylX* locus for 4 hr by the addition of 0.3% xylose. A strain that does not encode the Dendra2 was used as negative control (empty). (**B**) Immunoblots using antibodies to Dendra2 (top) or MreB (bottom, control) showing the abundance of the Dendra2-ZitP$^{1-43}$ variants from *R. sphaeroides* (Rs) in *C. crescentus WT* strains. Expression of Dendra2-ZitP$^{1-43}$ variants (WT, Q27R and Q27R/W35I double mutants) was induced from the *xylX* locus for 4 hr by the addition of 0.3% xylose. A strain that does not encode the Dendra2 was used as negative control (empty).

DOI: 10.7554/eLife.20640.007

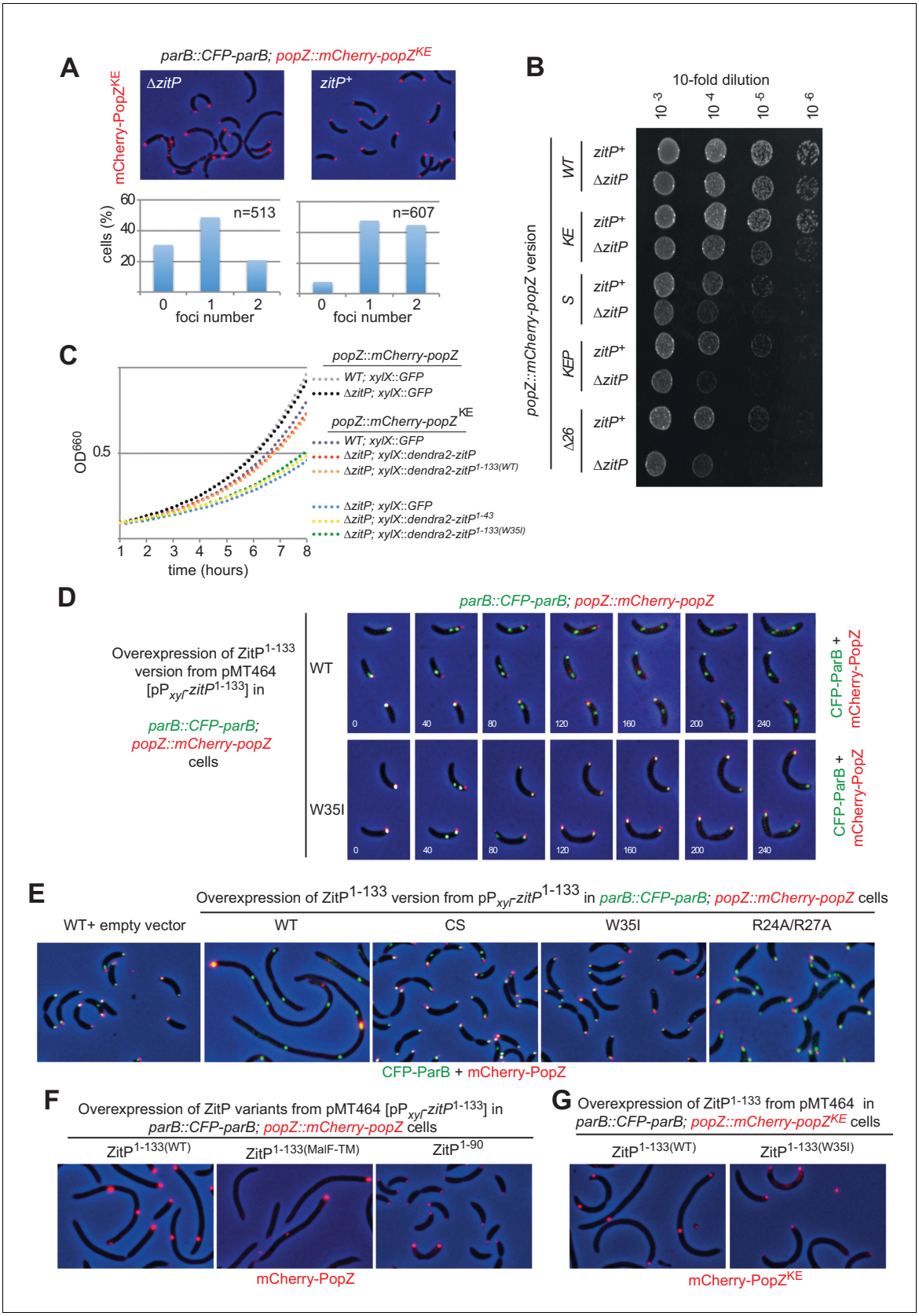

Figure 4. The ZitP•PopZ complex controls the *C. crescentus* cell division cycle. (**A**) Overlays of mCherry-fluorescence and phase contrast images of *WT* (upper panels) or Δ*zitP* (bottom) *C. crescentus* expressing the mCherry-PopZ^{KE} variant that no longer interacts with ParB. mCherry-PopZ^{KE} is expressed

Figure 4 continued on next page

Figure 4 continued

from the native locus (*mCherry-popZ*^{KE}) in lieu of untagged PopZ. Below the micrographs are quantifications of cells with and without bipolar or monopolar fluorescent foci of mCherry-PopZ^{KE}. (**B**) Efficiency of plating (EOP) assays of *C. crescentus* strains expressing *WT* mCherry-PopZ (*mCherry-popZ*) or variants that no longer interact with ParB (*mCherry-popZ*^{KE}), with ParA (*mCherry-popZ*^{SP}) or both (*mCherry-popZ*^{KEP} and *mCherry-popZ*$^{\Delta 26}$) in *WT* or Δ*zitP* cells. Serial ten-fold dilutions were plated on PYE agar containing spectinomycin. (**C**) Growth measurements of various strains monitored by optical density at 660 nm (OD660) in PYE. (**D**) Overlays of CFP- and mCherry-fluorescence with phase contrast images from *C. crescentus popZ::mCherry-popZ parB::CFP-parB* cells harbouring an empty plasmid (pMT464, left panel) or the pP$_{xyl}$-ZitP$^{1\text{-}133(WT)}$ derivative followed by time-lapse analysis with images acquired every 40 min. (**E**) Overlays of mCherry-fluorescence with phase contrast images from *C. crescentus popZ::mCherry-popZ parB::CFP-parB* cells harbouring an empty plasmid (pMT464, left panel) or derivatives: pP$_{xyl}$-ZitP$^{1\text{-}133(WT)}$ (second panel), pP$_{xyl}$-ZitP$^{1\text{-}133(CS)}$ (third panel), pP$_{xyl}$-ZitP$^{1\text{-}133(W35I)}$ (fourth panel) and pP$_{xyl}$-ZitP$^{1\text{-}133(R24A/R27A)}$ (right panel). Overexpression of ZitP$^{1\text{-}133}$ variants was induced with xylose 0.3% for 6 hr prior to imaging. (**F**) Overlays of mCherry-fluorescence with phase contrast images from *C. crescentus popZ::mCherry-popZ parB::CFP-parB* cells harbouring a P$_{xyl}$-ZitP$^{1\text{-}133(MalF\text{-}TM)}$, P$_{xyl}$-ZitP$^{1\text{-}133(WT)}$ or a P$_{xyl}$-ZitP$^{1\text{-}90}$ overexpression plasmid. Overexpression was induced by growth in 0.3% xylose for 6 hr prior to imaging. (**G**) Overlays of mCherry-fluorescence with phase contrast images from *C. crescentus popZ::mCherry-popZ*^{KEP} *parB::CFP-parB* cells harbouring a P$_{xyl}$-ZitP$^{1\text{-}133(WT)}$ or a P$_{xyl}$-ZitP$^{1\text{-}133(W35I)}$ overexpression plasmid. Overexpression was induced by growth in 0.3% xylose for 6 hr prior to imaging.

DOI: 10.7554/eLife.20640.008

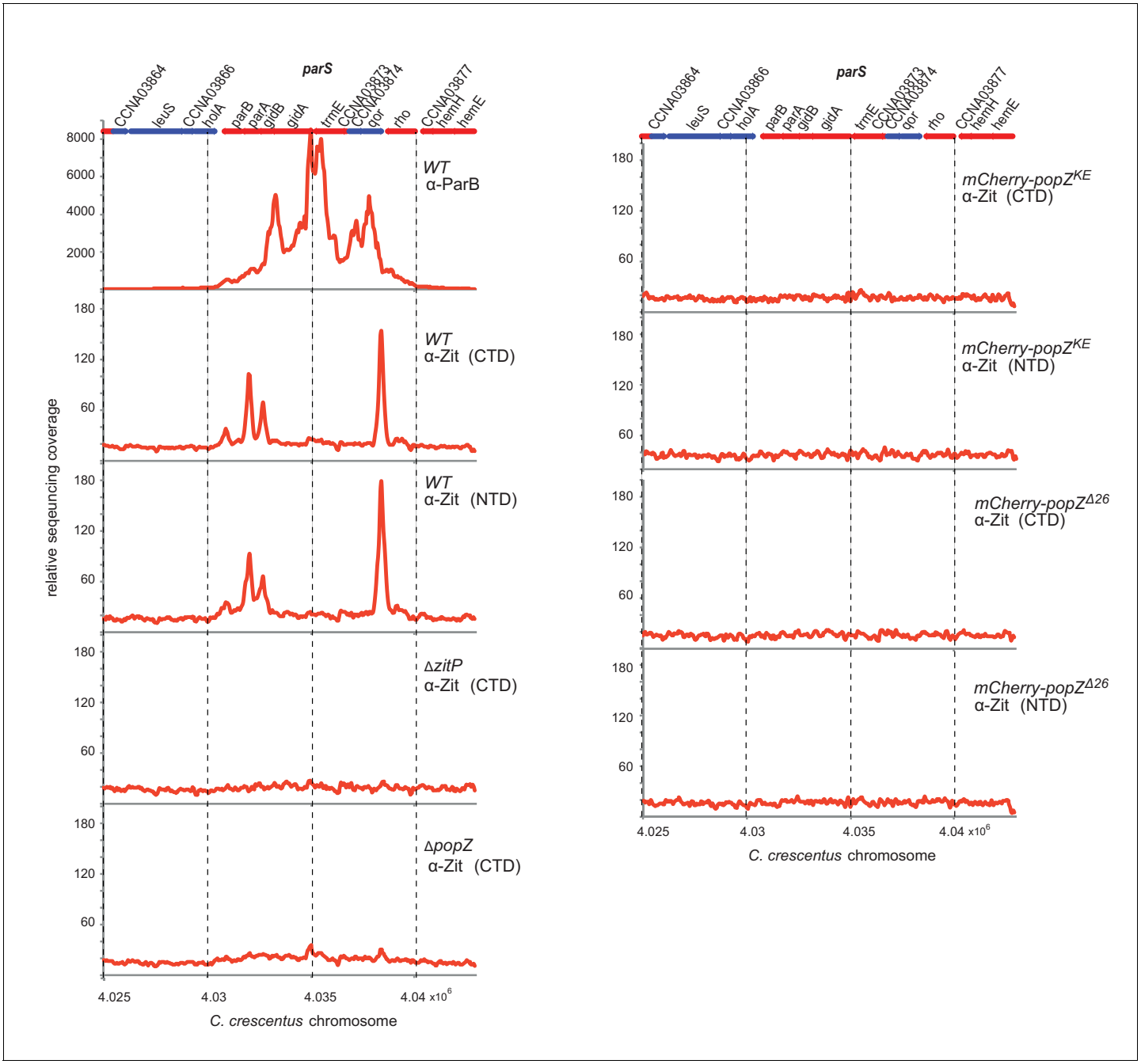

Figure 4—figure supplement 1. ChIP-Seq analysis of ZitP. Genome-wide occupancies of ParB in *WT* cells and ZitP in *WT*, Δ*zitP* and *popZ* mutant cells as determined by ChIP-Seq using antibodies to ParB (α-ParB) and different antibodies to (the N-terminal and C-terminal domains of) ZitP [α-ZitP(NTD) and α-ZitP(CTD), respectively]. The *x* axis denotes the nucleotide position on the genome, whereas the *y* axis denotes the relative abundance of reads for each probe (see Supplementary Methods for detailed description). Note that only the region from nucleotide 4,025,000 to 4,045,000 of the *C. crescentus WT* (NA1000) genome containing the *parS* centromere region is shown. Genes encoded from right to left are shown as blue bars, whereas the red bars indicate genes on the reverse strand. The numbers above the coding sequences refer to the CCNA gene annotation (***Marks et al., 2010***).
DOI: 10.7554/eLife.20640.009

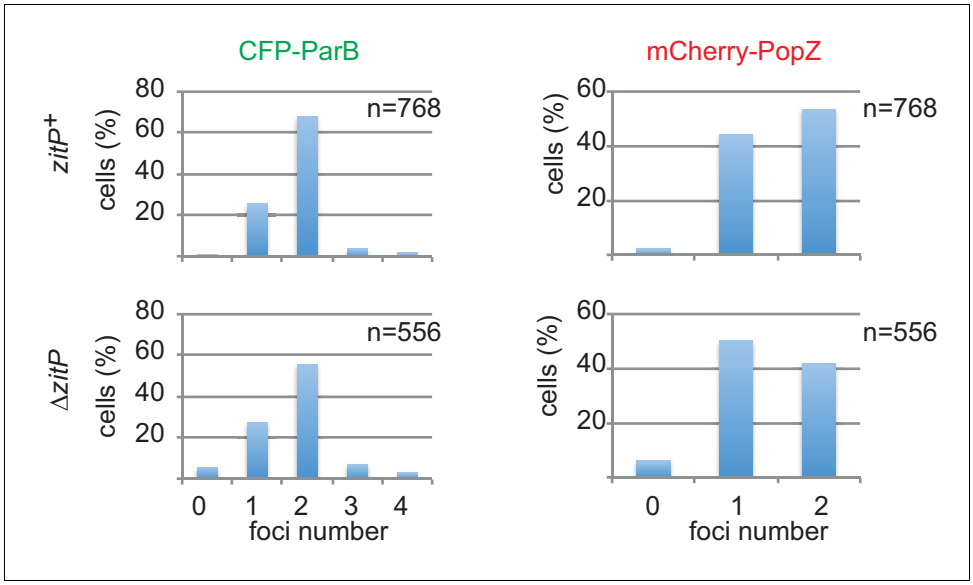

Figure 4—figure supplement 2. Quantification of polar CFP-ParB and mCherry-PopZ in *C.crescentus WT* and mutants. Quantification of CFP-ParB and mCherry-PopZ localization in *zitP*$^{+}$ or Δ*zitP* strains expressing CFP-ParB in lieu of untagged ParB from the *parB* locus and mCherry-PopZ from the *popZ* locus in lieu of native PopZ.
DOI: 10.7554/eLife.20640.010

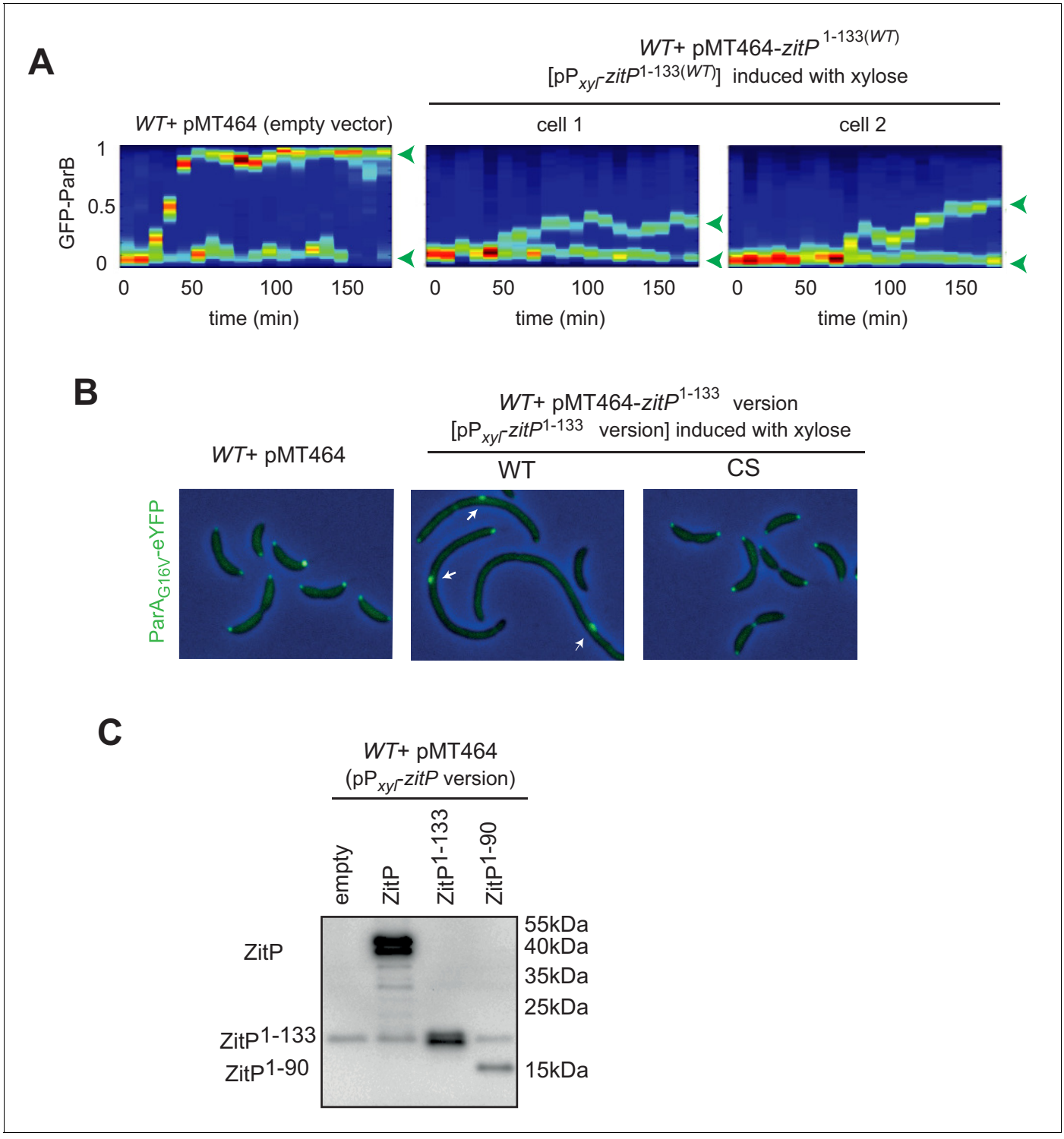

Figure 4—figure supplement 3. Localization of ParB and ParA upon ZitP$^{1-133}$ overexpression in *C.crescentus*. (**A**) Kymograph showing GFP-ParB localization along the *C. crescentus* cell cycle in *WT* or ZitP$^{1-133}$ overproduction. Swarmer (G1-phase) cells harbouring an empty plasmid or overexpressing ZitP$^{1-133(WT)}$ were cultivated in M2G before synchronization and transferred onto an agarose pad containing 0.3% xylose (t = 0 min) to induce ZitP$^{1-133}$, and visualized at 20 min intervals by light and fluorescence microscopy, respectively. Images were analysed using the kymograph tool from Microbe tracker. One representative cell from the *parB::GFP-parB* strain harbouring the empty plasmid is shown as well as two representative cells from the *parB::GFP-parB* strain overexpressing ZitP$^{1-133}$. Green arrowheads indicate the localization of GFP-ParB according to the cell length. (**B**) Images of *C. crescentus* harbouring an empty plasmid (pMT464, top panel), pP$_{xyl}$-ZitP$^{1-133(WT)}$ (middle panel), pP$_{xyl}$-ZitP$^{1-133(CS)}$ (bottom panel) and expressing from the chromosomal *xylX* locus a ParA$_{G16V}$-eYFP (dimerization deficient mutant which localize preferentially at the cell pole rather than

Figure 4—figure supplement 3 continued on next page

Figure 4—figure supplement 3 continued

nucleoid)(***Ptacin et al., 2010***). ZitP$^{1-133}$ over-expression was induced by growth in xylose 0.3% for 6 hr prior to imaging. Overlays between phase contrast and YFP-fluorescence images are shown. (**C**) Immunoblot showing the steady-state levels of *C. crescentus* ZitP or ZitP derivatives expressed from P_{xyl} on pMT464 in *C. crescentus WT* cells. *WT* harbouring empty pMT464 was used as a control. The blot was probed with the polyclonal antibody to the ZitP N-terminal domain (NTD). Note that endogenous ZitP expressed form the *zitP* locus is not detectable on this exposure due to the strong overproduction of the ZitP variants from the high copy plasmid.

DOI: 10.7554/eLife.20640.011

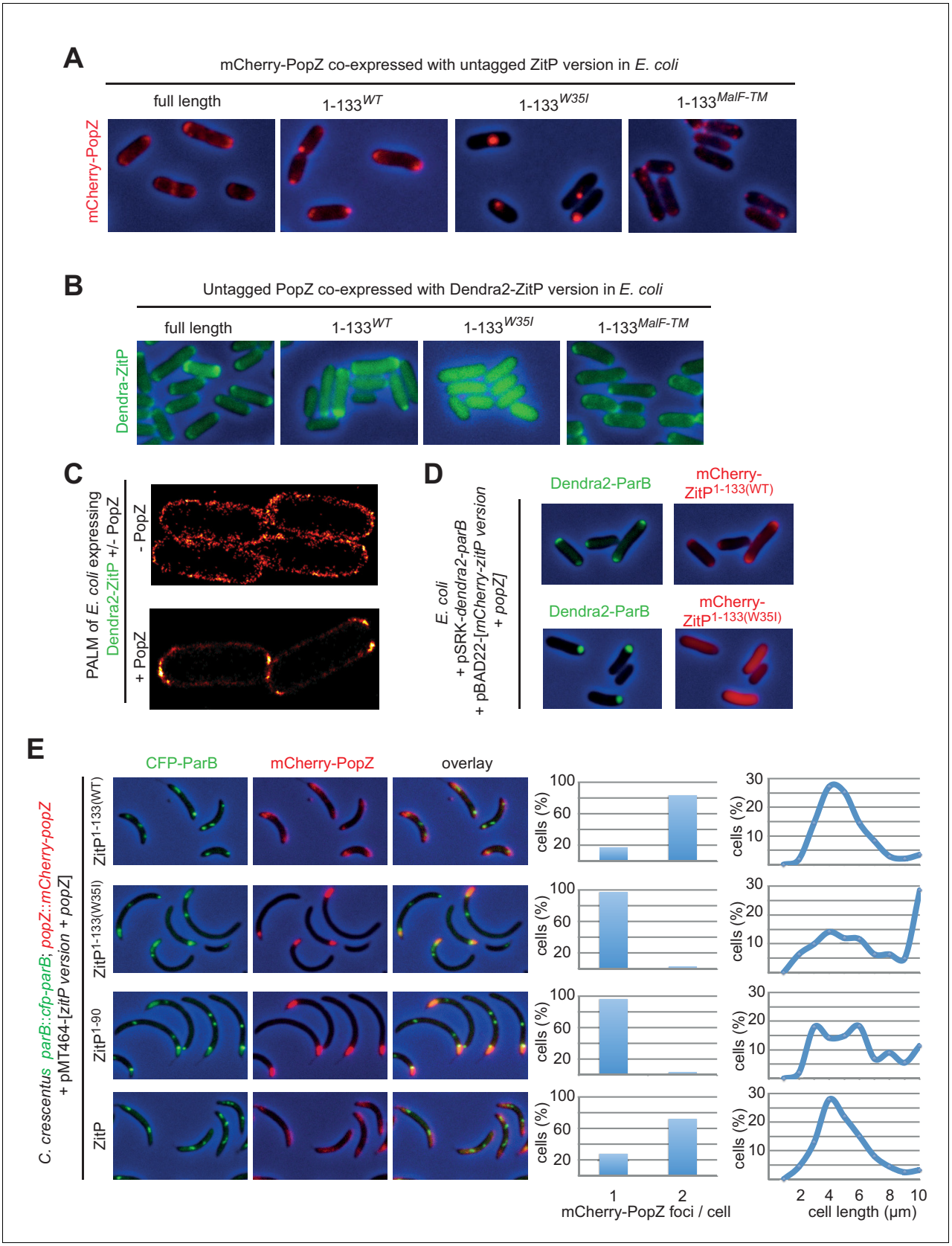

Figure 5. ZitP controls PopZ bipolarity in *E. coli* and *C. crescentus*. (**A**) Overlays of mCherry-fluorescence with phase contrast images of *E. coli* TB28 cells co-expressing mCherry-PopZ and various (untagged) ZitP versions: full length ZitP, or the derivatives ZitP$^{1-133}$, ZitP$^{1-133(W35I)}$ and ZitP$^{1-133(MalF-TM)}$.

Figure 5 continued on next page

Figure 5 continued

Cells were grown in LB for 2 hr, then ZitP variants and mCherry-PopZ were induced with 1 mM IPTG and 0.2% L-arabinose, respectively, for 2 hr before imaging. (**B**) Overlays of Dendra2-fluorescence with phase contrast images of *E. coli* TB28 cells co-expressing (untagged) PopZ and full length Dendra2-ZitP, Dendra2-ZitP$^{1\text{-}133(WT)}$, Dendra2-ZitP$^{1\text{-}133(W35I)}$ or Dendra2-ZitP$^{1\text{-}133(MalF\text{-}TM)}$. Cells were grown in LB for 2 hr, then Dendra2-ZitP and mCherry-PopZ were induced with 1 mM IPTG and 0.2% L-arabinose, respectively, for 2 hr before imaging. (**C**) PALM (photo-activated localization microscopy) images of *E. coli* cells expressing Dendra2-ZitP from pSRK-Km (***Khan et al., 2008***) and either no PopZ (empty pBAD101(***Guzman et al., 1995***) vector, strain EC127, left panel) or untagged PopZ from pBAD101 (strain EC132, right panel). (**D**) Overlays of Dendra2- and mCherry-fluorescence with phase contrast images showing the co-localization of Dendra2-ParB (from P_{lac} on pSRK-Km) with WT or W35I mCherry-ZitP$^{1\text{-}133}$ derivatives in *E. coli* cells co-expressed with untagged PopZ from P_{ara} on pBAD22. (**E**) Overlays of CFP- and/or mCherry-fluorescence with phase contrast images of *C. crescentus popZ::mCherry-popZ parB::CFP-parB* cells co-overexpressing (untagged) full-length ZitP, ZitP$^{1\text{-}90}$, ZitP$^{1\text{-}133(W35I)}$ or ZitP$^{1\text{-}133(WT)}$ with (untagged) PopZ under P_{xyl} control from pMT464. Over-expression was induced by growth in xylose 0.3% for 4 hr prior to imaging. mCherry-PopZ (upper panel) and CFP-ParB (middle panel) are expressed from their native promoters at the respective endogenous chromosomal loci in lieu of the untagged form.

DOI: 10.7554/eLife.20640.012

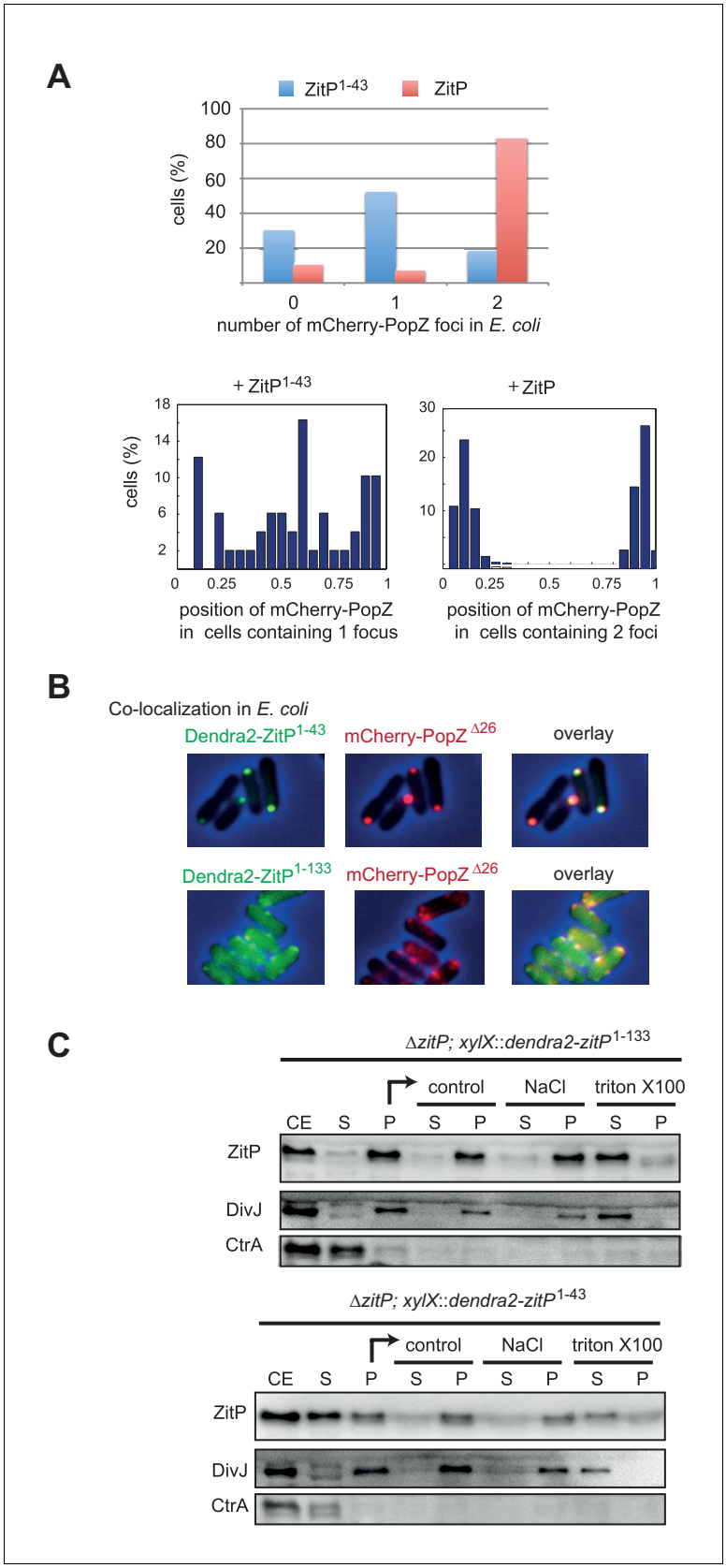

Figure 5—figure supplement 1. Co-localization of ZitP and PopZ in *E.coli*. (**A**) Quantification of mCherry-PopZ localization in *E. coli* cells co-expressing mCherry-PopZ and Dendra2-ZitP$^{1-43}$ or Dendra2-ZitP. The top panel

Figure 5—figure supplement 1 continued on next page

Figure 5—figure supplement 1 continued

indicates the number of PopZ foci per cell when mCherry-PopZ is co-expressed with Dendra2-ZitP$^{1-43}$ (blue) (n = 151) or Dendra2-ZitP (red) (n = 502). The bottom left and right panels show the relative position of foci (n = 502) along longitudinal axis of mCherry-PopZ foci in cells co-expressing Dendra2-ZitP$^{1-43}$ (middle, for cells having one focus) or Dendra2-ZitP (right, for cells having two foci). Position 0 reflects one pole and position one the opposite pole. (**B**) *C. crescentus* PopZ$^{\Delta 26}$ still interacts with *C. crescentus* ZitP in *E. coli*. Overlays of Dendra2- and/or mCherry-fluorescence with phase contrast images of *E. coli* TB28 cells expressing Dendra2-ZitP$^{1-43}$ (left, upper panel) or Dendra2-ZitP$^{1-133}$ (left, bottom panel) in the presence of mCherry-PopZ (middle panel). Co-localized red and green foci appear yellow in the overlay (right panel). Cells were grown in LB media for 2 hr, then expression of Dendra2-ZitP$^{1-43}$ variants and mCherry-PopZ was induced with 1 mM IPTG and 0.2% L-arabinose, respectively, for 2 hr. (**C**) Biochemical fractionation of ZitP from extracts of cells expressing Dendra2-ZitP$^{1-133}$ or Dendra2-ZitP$^{1-43}$. Expression of Dendra2-ZitP$^{1-43}$ or Dendra2-ZitP$^{1-133}$ integrated at the chromosomal *xylX* locus was induced for 4 hr by the addition of 0.3% xylose. The cells were lysed by sonication (CE, cell extract) and the soluble fraction (**S**) was separated from the membrane fraction (pellet, **P**) by centrifugation. This fraction (**P**) was taken up in re-suspension buffer (control) with or without a 2 M NaCl final buffer (NaCl) or 1% Triton X-100 (Triton X-100). After centrifugation, the soluble fraction (**S**) and insoluble fraction (**P**) were collected. All the fractions were analysed by immunoblotting using antibodies to the ZitP (NTD) (top), DivJ as a membrane protein control (middle panel) and CtrA as a soluble protein control (bottom panel).

DOI: 10.7554/eLife.20640.013

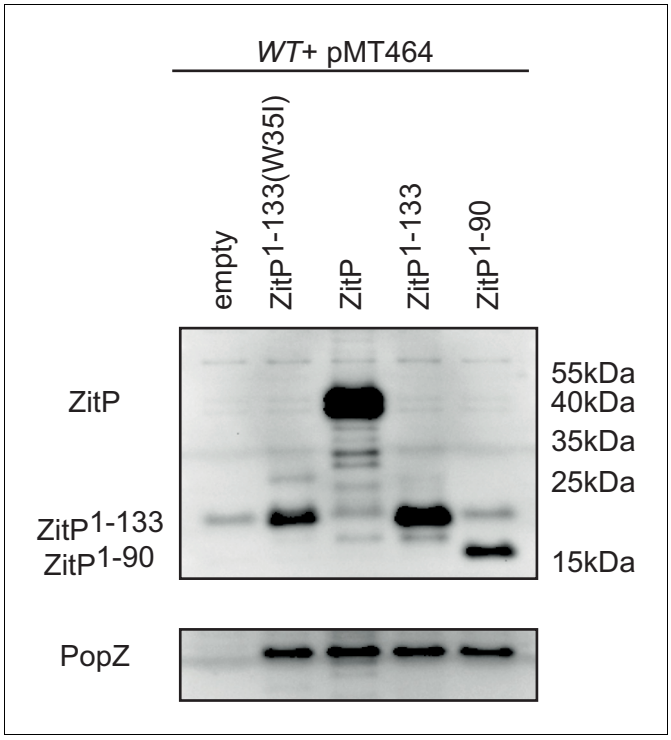

Figure 5—figure supplement 2. Steady-state levels of PopZ and ZitP variants upon co-overexpression in *C. crescentus*. Immunoblots showing the steady-state levels of *C. crescentus* ZitP or ZitP derivatives co-expressed with *C. crescentus* PopZ from P_{xyl} on pMT464 in *C. crescentus WT* cells. *WT* harbouring empty pMT464 was used as a control. The blot shown in the top panel was probed with polyclonal antibodies to the ZitP N-terminal domain (NTD). The blot in the lower panel shows the same blot re-probed with the polyclonal antibodies to PopZ. Note that endogenous ZitP and PopZ expressed from the *zitP* and *popZ* locus, respectively, are not detectable on this exposure due to the strong overproduction of the ZitP variants and PopZ from the high-copy plasmid.
DOI: 10.7554/eLife.20640.014

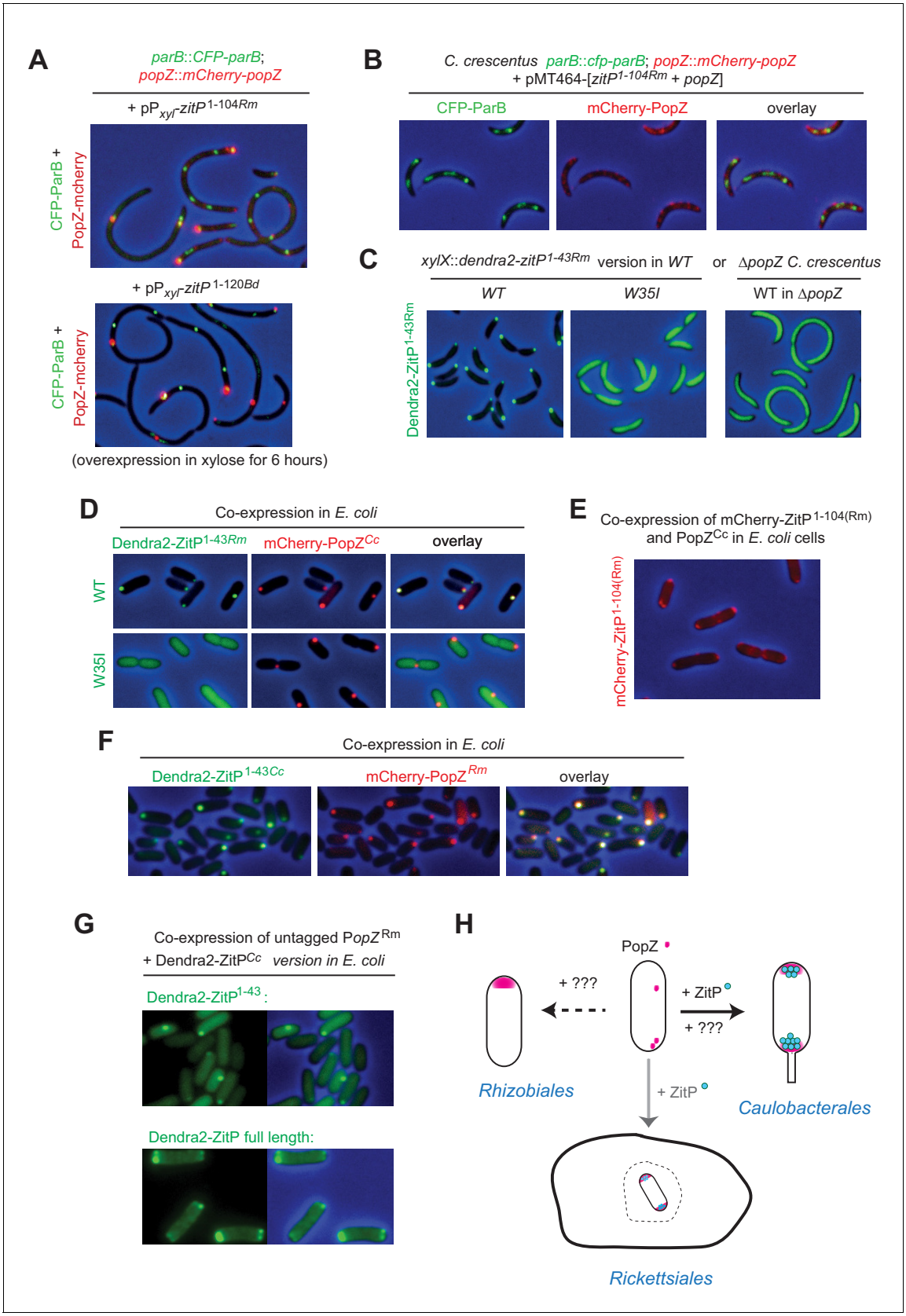

Figure 6. Conservation of PopZ•ZitP localization and activity (**A**) Overlays of CFP- and mCherry-fluorescence with phase contrast images of *C. crescentus popZ::mCherry-popZ parB::CFP-parB* cells over-expressing ZitP$^{1-104}$ from *R. massiliae* (upper panel) or *B. diminuta* (lower panel) from P_{xyl} on

Figure 6 continued on next page

Figure 6 continued

a multi-copy plasmid (pMT464). mCherry-PopZ and CFP-ParB are expressed from the chromosome in lieu of the untagged versions. ZitP$^{1-104}$ over-expression was induced by the addition of 0.3% xylose for 6 hr prior to imaging. (**B**) Overlays of CFP- and mCherry-fluorescence with phase contrast images of *C. crescentus popZ::mCherry-popZ parB::CFP-parB* cells over-expressing ZitP$^{1-104}$ from *R. massiliae* with *C. crescentus* PopZ. Over-expression was induced by the addition of 0.3% xylose for 6 hr prior to imaging. (**C**) Overlays of Dendra2-fluorescence with phase contrast images of the *R. massiliae* (Rm) ZitP ZnR version expressed from the *xylX* locus in *WT* and Δ*popZ C. crescentus* cells. Synthesis of the Dendra2-ZitP$^{1-43(WT)Rm}$ or Dendra2-ZitP$^{1-43(W35I)\ Rm}$ was induced for 4 hr with 0.3% xylose before imaging. (**D**) Overlays of Dendra2- and/or mCherry-fluorescence with phase contrast images of *E. coli* TB28 cells expressing *R. massiliae* (Rm) Dendra2-ZitP$^{1-43(WT)}$ (upper panels), Dendra2-ZitP$^{1-43(W35I)}$ (lower panel) in the presence of mCherry-tagged PopZ from *C. crescentus*. Cells were grown in LB for 2 hr, then Dendra2-ZitP$^{1-43}$ variants and mCherry-PopZ were induced with 1 mM IPTG and 0.2% L-arabinose, respectively, for 2 hr. (**E**) Overlay of mCherry-fluorescence with phase contrast images of *E. coli* TB28 cells co-expressing mCherry-ZitP$^{1-104Rm}$ from *R. massiliae* (Rm) with *C. crescentus* PopZ from P_{ara} encoded on the same pBAD22-derived plasmid. Cells were grown in LB for 2 hr, then expression of mCherry-ZitP$^{1-104Rm}$ and PopZ was induced with 0.2% L-arabinose for 2 hr before imaging. (**F**) Overlays of Dendra2- and/or mCherry-fluorescence with phase contrast images of *E. coli* TB28 cells expressing *C. crescentus* Dendra2-ZitP$^{1-43}$ (Cc) in the presence of mCherry-PopZ from *R. massiliae* (Rm). Cells were grown in LB for 2 hr, then Dendra2-ZitP$^{1-43}$ and mCherry-PopZ were induced with 1 mM IPTG and 0.2% L-arabinose, respectively, for 2 hr. (**G**) Images of *E. coli* cells co-expressing *C. crescentus* Dendra2-ZitP$^{1-43}$ (Cc, upper panel) or Dendra2-ZitP full-length (Cc, bottom panel) and PopZ from *R. massiliae* (Rm). Fluorescence (Dendra2) images (left panels) and overlays between phase contrast and Dendra2 fluorescence images (right panels) are shown. Cells were grown in LB to during 2 hr, then Dendra2-ZitP$^{1-43}$ variants were induced with 1 mM IPTG and PopZ was induced with 0.2% L-arabinose for 2 hr. (**H**) The (bi)polar PopZ•ZitP complex of free-living (Caulobacterales) and obligate intracellular (Rickettsiales) α-proteobacteria. Pink dots denote PopZ monomers that assemble into a bipolar or monopolar patch, while blue dots denote ZitP molecules. An obligate intracellular rickettsial (rod with bipolar PopZ) cell is depicted within a vacuole (dashed structure) of a host cell (closed structure) and presumed also to polarize PopZ•ZitP (grey arrow). As ZitP is not present in the Rhizobiales, another mechanism of PopZ control is likely operational to drive it into a monopolar disposition. Similarly, we suggest that PopZ localization in *C. crescentus* can be accomplished by another pathway that operates independently of ZitP and likely involves ParAB and/or another pathway (see Discussion).

DOI: 10.7554/eLife.20640.015